

Integrated Digital Microfluidic Platform for Voltammetric Analysis

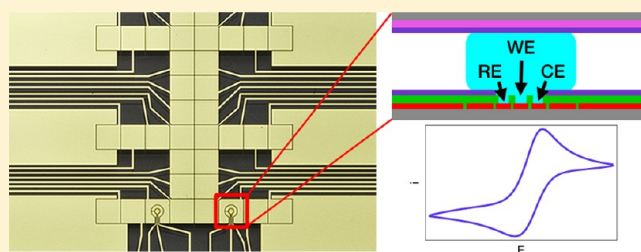
Michael D. M. Dryden,[†] Darius D. G. Rackus,[†] Mohtashim H. Shamsi,[†] and Aaron R. Wheeler^{*,†,‡,¶}

[†]Department of Chemistry, University of Toronto, 80 St. George Street, Toronto, Ontario M5S 3H6, Canada

[‡]Institute for Biomaterials and Biomedical Engineering, University of Toronto, 164 College Street, Toronto, Ontario M5S 3G9, Canada

[¶]Donnelly Centre for Cellular and Biomolecular Research, 160 College Street, Toronto, Ontario M5S 3E1, Canada

ABSTRACT: Digital microfluidics (DMF) is an emerging technique for manipulating small volumes of liquids. DMF is particularly well suited for analytical applications as it allows automated handling of discrete samples, and it has been integrated with several inline analysis techniques. However, examples of the integration of DMF with electroanalytical methods are notably scarce, and those that have been reported rely on external electrodes that impose limitations on complexity. To combine the full capabilities of DMF with voltammetry, we designed a platform featuring a three-electrode electrochemical cell integrated in a microfabricated DMF device, removing the need for external electrodes and allowing for complete droplet control. The performance of the DMF/voltammetry system is comparable to that of a commercial screen printed electrode, and the new platform was applied to generating a calibration series for acetaminophen with a limit of detection of 76 μM and good precision (4% average RSD), all with minimal human intervention. We propose that this platform and variations thereof may be a useful new tool for microscale electroanalysis and will be a complementary system to existing inline analysis techniques for DMF.



Digital microfluidics (DMF) is a miniaturized fluid-handling technique used to manipulate nanoliter to microliter volumes of liquids. In contrast to the serial addressing of systems relying on microchannels, in DMF, droplets can be actuated independently and in parallel across a grid of electrodes coated with a hydrophobic dielectric. Droplets are moved in a defined path by sequential application of an electrical potential to electrodes on the device, the product of an electromechanical force exerted by the accumulation of charges or dipoles at the interface of the device and droplet surfaces.¹ The main advantages of DMF include the ability to handle small samples, the freedom from diffusion limits to mixing times, the ability to address fluids as individual droplets rather than a continuous flow, and the capacity for automation and multiplexing.² With these capabilities being applied to synthetic chemistry,³ chemical biology,⁴ and sample preparation,⁵ techniques for the analysis of droplet contents are of particular interest.

Inline analysis techniques, where detection can be performed directly in the droplets on a DMF device, are desirable because they minimize the complexity of an experiment and can allow real-time monitoring of chemical changes occurring within the droplets. A number of inline analysis techniques have been coupled with DMF, including absorbance detection,⁶ fluorescence and chemiluminescence,⁷ surface plasmon resonance,⁸ and mass spectrometry.⁹ These are useful advances, but each of these modes has strengths and weakness. For example, absorbance detection can be implemented with inexpensive, small footprint instrumentation, but it has limited sensitivity and provides limited qualitative information. Fluorescence and

chemiluminescence are very sensitive but require the use of labels or a restricted set of applicable analytes. Surface plasmon resonance offers label-free detection but lacks selectivity without surface functionalization. Mass spectrometry provides a useful combination of sensitivity and qualitative information but requires sizable and costly instrumentation.

We propose that voltammetric analysis offers a balance between the sensitivity and selectivity of mass spectrometry and the simple, economical instrumentation of absorbance detection. Voltammetry has a number of advantages including high sensitivity, label and label-free detection of a wide variety of analytes, and relatively compact and inexpensive instrumentation. It seems well suited for integration with DMF because the steps required to form electrodes for droplet actuation are similar to those required to form electrodes for electrochemical detection. To our knowledge, there have been only two reports describing the combination of voltammetry with DMF.^{10,11} These previous reports represent a useful step forward, but the methods suffer from key limitations, including: (a) the devices were formed in “single-plate” DMF format, meaning that they are incapable of droplet splitting or dispensing from reservoirs; and (b) the voltammetric analysis electrodes in these preliminary reports were not integrated into the device (i.e., free-standing wire-electrodes were inserted into the droplets from above). We hypothesized that a sophisticated, practical system could be developed by combining the “two-plate” DMF

Received: July 2, 2013

Accepted: August 8, 2013

Published: September 3, 2013

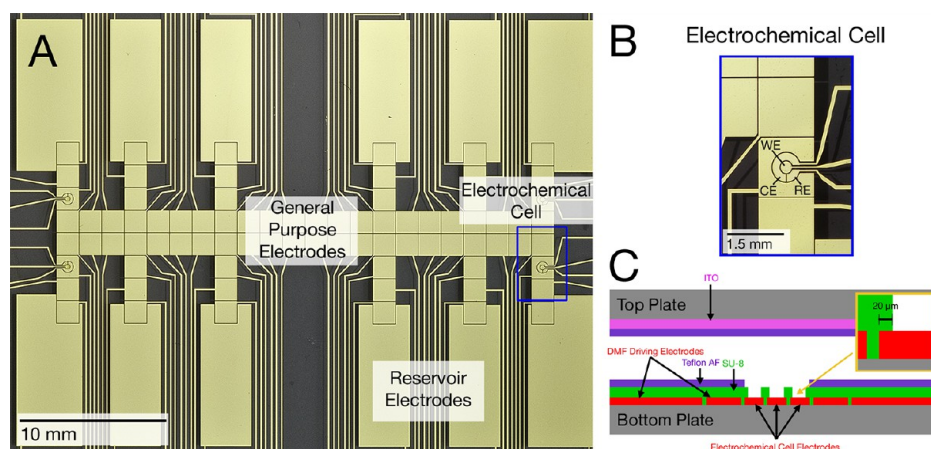


Figure 1. DMF device for integrated voltammetric analysis. (A) Picture of a device. (B) Magnified image of one of the electrochemical cells, with labeled working electrode (WE), reference electrode (RE) and counter electrode (CE). (C) Side-view schematic of an electrochemical cell, with labeled Au electrode layer (red), SU-8 dielectric layer (green), Teflon AF hydrophobic layers (purple), and ITO conductive layer (magenta). As shown in the inset, the SU-8 was patterned such that it extended over the edge of each cell electrode, effectively sealing the edges from contact with liquids.

format (allowing for complex droplet operations such as dispensing from reservoirs) with integrated voltammetric electrodes for straightforward system setup and operation.

Here we describe the design, fabrication, and use of the first two-plate DMF platform for microscale fluid manipulation and integrated, inline voltammetric analysis. The electroanalytical performance was characterized and compared with that of a commercially available screen-printed electrode chip. The system was validated by application to on-chip generation of a dilution series of a model analyte, acetaminophen, featuring analyses with high precision (4% average RSD) and a limit of detection of $76 \mu\text{M}$. This platform expands the palette of analysis techniques available for use with DMF and provides a system for low-volume voltammetric experiments with reduced manual handling.

EXPERIMENTAL SECTION

Reagents and Materials. Unless otherwise noted, chemicals and reagents were purchased from Sigma-Aldrich (St. Louis, MO). Teflon AF 1600 was purchased from DuPont (Wilmington, DE). DRP-223AT disposable screen printed electrodes with gold working and auxiliary electrodes and a silver pseudoreference electrode were purchased from Drop-Sens (Llanera, Spain). Gold-coated glass substrates (100 nm Au over 20 nm Cr as adhesion layer) were obtained precoated with AZ1500 positive photoresist from Telic Company (Valencia, CA). Indium-doped tin oxide-coated (ITO) glass slides were purchased from Delta Technologies, Ltd. (Loveland, CO). SU-8 3005 negative photoresist and SU-8 developer were from MicroChem Corp. (Newton, MA), Microposit MF-321 developer and S1811 positive photoresist were from Rohm and Haas (Marlborough, MA), AZ 300T stripper was from AZ Electronic Materials (Somerville, NJ), and CR-4 chromium etchant was from Cyantek (Fremont, CA). Transparent photomasks were printed at 20,000 DPI by Pacific Arts and Designs Inc. (Markham, ON). All solutions actuated by DMF contained 0.05% Pluronic F-68.

Device Fabrication. DMF devices were fabricated at the University of Toronto Nanofabrication Centre (TNFC), using standard microfabrication techniques. To form DMF bottom plates, photoresist-coated gold-on-glass substrates were pat-

terned by exposure to UV through a photomask using a Suss MicroTec mask aligner ($29.8 \text{ mW}/\text{cm}^2$, 10 s), developed in MF-321 developer for 60 s, and then etched in gold etchant for 30 s followed by immersion in CR-4 chromium etchant for 45 s. The remaining photoresist was stripped using AZ 300T stripper, and the substrate was rinsed successively with acetone, isopropyl alcohol, and deionized water and then dried on a hot plate at $95 \text{ }^\circ\text{C}$. As shown in Figure 1A, the pattern comprised 92 DMF electrodes (separated from each other by $30 \mu\text{m}$), including 8 reagent reservoirs ($3.4 \times 9.7 \text{ mm}$), 4 waste reservoirs (42 mm^2), and 80 square actuation electrodes ($1.5 \times 1.5 \text{ mm}$). Each DMF electrode was connected by a $100 \mu\text{m}$ thick patterned wire to an electrode in an array of $1 \times 1 \text{ mm}$ pogo-pin contact pads at the sides of the substrate. As shown in Figure 1B, four of the square DMF actuation electrodes were modified to contain an electrochemical cell insert, including a $150 \mu\text{m}$ radius circular working electrode surrounded by an annular region of $180 \mu\text{m}$ inner radius and $370 \mu\text{m}$ outer radius containing working ($\sim 270^\circ$ of annulus) and reference ($\sim 90^\circ$ of annulus) electrodes. Each cell electrode was connected by a $100 \mu\text{m}$ thick patterned wire to an electrode in an array of rectangular pads spaced at 1.27 mm for connection with an SOIC test clip.

An $8 \mu\text{m}$ thick layer of SU-8 3005 was applied to patterned gold-on-glass substrates by spin coating at 2000 rpm followed by baking on a hot plate at $95 \text{ }^\circ\text{C}$ for 5 min. Apertures through the SU-8 were formed by exposing to UV through a photomask (22 s), baking for 5 min at $95 \text{ }^\circ\text{C}$, and then developing in SU-8 developer for 5 min. Substrates were rinsed successively with acetone, isopropyl alcohol, and deionized water and then dried at $95 \text{ }^\circ\text{C}$. As shown in Figure 1C, each aperture was slightly smaller than a corresponding electrochemical cell electrode, and the apertures were aligned such that SU-8 extended $\sim 20 \mu\text{m}$ over the edges of each cell electrode. Finally, a $\sim 200 \text{ nm}$ thick layer of Teflon-AF 1600 was applied and patterned with $370 \mu\text{m}$ radius apertures using an adaptation of the lift-off technique described previously for ITO-coated substrates,¹² omitting the RCA solution pretreatment, reducing the bake temperature after Teflon application to $145 \text{ }^\circ\text{C}$, and performing only a single post lift-off bake at $165 \text{ }^\circ\text{C}$ for 5 min. As depicted in Figure 1C, the completed bottom plate was thus globally

coated with SU-8 and Teflon-AF, with apertures opened only over the electrochemical cell electrodes.

Some DMF bottom plates were modified such that the reference electrodes in the electrochemical cell were coated with silver. Briefly, a 100 μL aliquot of a 300 mM solution of AgNO_3 in 1 M NH_4OH was pipetted onto each electrochemical cell. A potential difference of -0.8 V was applied between the reference electrode and an external stainless steel counter electrode for 5 s, using a regulated DC power supply. The liquid was removed, and the cell was rinsed with deionized water. DMF top plates were formed from unpatterned ITO-coated glass substrates coated with ~ 200 nm thick Teflon AF 1600 as described previously.¹³ After fabrication, device top and bottom plates were stored in a sealed chamber with a desiccant until use.

Device Assembly and Operation. Each DMF device was assembled from a bottom plate and a top plate separated by spacers created from two pieces of 3M Scotch double-sided tape (St. Paul, MN) with a total spacer thickness of 180 μm . With this geometry, unit droplets (i.e., those that cover a single square actuation electrode) were ~ 400 nL. The open-source DropBot DMF control system (described in detail elsewhere¹⁴) was used to program and manage droplet movement. Briefly, droplet actuation was achieved by applying sine wave voltages (~ 100 V_{rms}, 10 kHz) between the top plate electrode and successive electrodes on the bottom plate via a custom pogo-pin connector. Droplet movement was monitored and recorded with a Vixia HF200 video camera (Canon, Japan).

Voltammetric Characterization and Analysis. Electrochemical cell electrodes were cleaned, and voltammetric measurements were made using an EmStat MUX8 potentiostat (PalmSens BV, Utrecht, NL) attached to devices using an SOIC clip. Briefly, for cleaning, a 100 μL aliquot of a 0.5 M solution of H_2SO_4 was pipetted onto each DMF electrochemical cell. The electrodes were subjected to 20 cycles of cyclic voltammetry (CV) between 300 mV and 1300 mV at a scan rate of 400 mV/s. Repeated oxidation and reduction of the working electrode surface was observed, and the oxide reduction peak of the final scan was used to estimate the surface area of the working electrode by the oxygen adsorption method, using the reference charge density for polycrystalline gold of 390 $\mu\text{C}/\text{cm}^2$.¹⁵ To characterize electrochemical cell performance, 100 μL aliquots of 5 mM potassium hexacyanoferrate(III) in pH 7 McIlvaine buffer¹⁶ were pipetted onto either a DMF electrode cell or a DRP-223AT screen-printed electrode. Each aliquot was allowed to equilibrate for 5 min, and CV measurements were made from 400 mV to -200 mV at scan rates varying from 10 to 100 mV/s. For integrated DMF experiments, acetaminophen standards were evaluated by linear sweep voltammetry from 200 to 800 mV at a scan rate of 70 mV/s.

Multistep Analysis of Acetaminophen. Multistep sensing experiments were performed in 8 steps. In step (1), one 6 μL aliquot each of standard solution (2 or 10 mM acetaminophen in pH 3 McIlvaine buffer) and diluent (pH 3 McIlvaine buffer) were loaded into their respective reservoirs. In step (2), two successive (identical) unit droplets of standard solution were dispensed from their reservoir, driven to the electrochemical cell, and then driven to waste. In step (3), a third (identical) unit droplet of standard solution was dispensed from the reservoir, moved to the electrochemical cell, and allowed to equilibrate for 120 s prior to analysis by linear sweep voltammetry (as above). In step (4), a unit droplet

of diluent was dispensed from a reservoir and merged with the droplet containing acetaminophen. The merged droplet was driven away from the electrochemical cell, actuated in a circular pattern in the general purpose electrode area, and then returned to the electrochemical cell. This mixing process was repeated twice, and, finally, the droplet was allowed to equilibrate for 180 s prior to analysis by voltammetry (as above). In steps (5–8), step (4) was repeated, forming and analyzing progressively diluted acetaminophen droplets.

Coincident with each voltammetric analysis, a high-resolution picture was collected and used to estimate the droplet volume. Briefly, the area of each droplet was identified using Photoshop CS3 Extended (Adobe, San Jose, CA), and the volume was estimated by multiplying the area by the interplate spacer distance. For the initial droplet (step 3), the volume was multiplied by the standard concentration to estimate the absolute amount of acetaminophen. For merged droplets (steps 4–8) the concentration was estimated by dividing the absolute amount of acetaminophen by the estimated merged droplet volume. The 8-step dilution curve generation and analysis process was replicated six times: three times each for 10 mM and 2 mM acetaminophen standards. Eight blank measurements (diluent only) were also collected. Average peak currents were plotted as a function of concentration and were fit with a linear regression. The limit of detection (LOD) and limit of quantitation (LOQ) were determined as the concentrations corresponding to the regression value equal to the average signal of the blank plus three (LOD) or ten (LOQ) standard deviations. Concentration variances were calculated using the propagation method described by Ku.¹⁷

RESULTS AND DISCUSSION

Device and Electrode Characterization. Digital microfluidic devices were produced bearing an array of driving electrodes coated with a hydrophobic insulator. The device design (Figure 1A) is superficially similar to one reported previously,¹⁸ but a key novelty was the inclusion of a series of three-electrode electrochemical cells (Figure 1B) that were exposed to droplets on the device (Figure 1C). To facilitate this, we used SU-8 as an insulator in place of the more commonly used Parylene C. In initial experiments, SU-8 was patterned with apertures such that each electrochemical cell electrode was completely exposed. This was found to be problematic, as the application of voltammetric potentials to cells formed in this manner caused the cell electrodes to delaminate (presumably a consequence of oxidation of the thin chromium adhesion layer), making them useless. This problem was solved by patterning the apertures through the SU-8 such that the polymer extended ~ 20 μm over each cell electrode edge (Figure 1C inset), protecting the adhesion layer from oxidation in solution. Devices formed in this manner did not suffer from delamination and could be used for many sequential experiments. Another potential solution for future work is the use of titanium (which resists oxidation more readily than chromium) as an adhesion layer for gold.

Prior to integrated digital microfluidic experiments, the performance of the new DMF/electrochemical cells was evaluated using cyclic voltammetry. Sulfuric acid was chosen as a model analyte, as it is commonly used for cleaning and characterizing gold electrodes.¹⁹ The principal phenomena observed in such experiments are the formation of an oxide monolayer on the gold surface on the forward scan and the

reduction of the surface to pure gold on the reverse scan. As described in the Experimental Section, the initial device design employed gold working, counter, and reference electrodes. Unfortunately, cyclic voltammograms generated using these electrochemical cells resulted in large shifts in peak potentials, (up to 40 mV between scans), indicating an unstable reference potential (Figure 2A). This is undesirable, as it complicates the

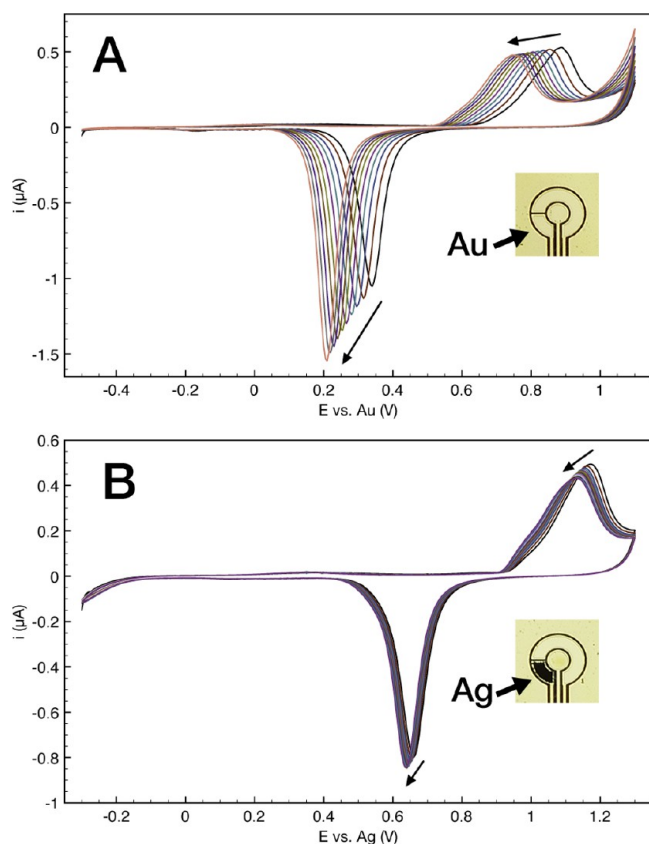


Figure 2. Comparison between Au and Ag pseudoreference electrodes on DMF devices. Cyclic voltammograms of 0.5 M H₂SO₄ at 400 mV/s with (A) Au reference electrode and (B) Ag reference electrode. Arrows point toward increasing scan numbers. Insets: pictures of voltammetric sensing areas featuring Au and Ag reference electrodes.

assignment of peaks and may also shift the measurement window out of the range of interest or into regions at which hydrogen or oxygen evolution occur.

In the all-gold electrochemical cell measurements described above, the reference electrode behaves as a pseudoreference (because there are no ionic gold species in solution), with a potential that depends on the composition of the solution and its interaction with the electrode surface.²⁰ Because silver has been shown to work well as a pseudoreference electrode material, perhaps as a consequence of low concentrations of redox couples in the measurement solution not present in the less easily oxidized gold, we hypothesized that a silver reference electrode would improve stability. As described in the Experimental Section, methods were developed to selectively electroplate silver onto the reference electrodes; these structures greatly improved performance, with reference potential drift of less than 2 mV between scans (Figure 2B). This level of stability is suitable for many electroanalytical experiments (and in addition, pseudoreference electrodes have the advantage of low impedance²⁰). The reference electrodes

were found to be stable after at least 2 weeks of dry storage and could be regenerated quickly by electrochemical stripping and redeposition, if necessary. If further enhancements are needed, they might be obtained by fabricating thin film Ag/AgCl reference²¹ or metal/polypyrrole quasireference²² electrodes. Regardless, silver-plated reference electrodes were used for all of the experiments described below.

Using silver-plated reference electrodes in 0.5 M H₂SO₄, the useful potential window for measurement was found to extend between approximately -0.2 V, where hydrogen evolution occurs, and +0.9 V, at the onset of oxygen adsorption. Because the oxygen adsorption peak (on the forward scan) overlapped the region for oxygen evolution, the gold oxide stripping peak (on the reverse scan) was used to estimate the effective surface area of the working electrode. The effective surface area was found to be 0.064 ± 0.005 mm² (average ± SD for *n* = 8), compared to the geometric surface area of 0.053 mm² assuming a planar circular electrode with the same dimensions (accounting for the 20 μm SU-8 border around the electrode). The small increase in effective surface area relative to geometric area may be a result of nonvertical SU-8 walls (exposing a greater-than-anticipated area of the electrode surface), or it may be a function of surface roughness associated with the gold coating process or introduced by the repeated electrochemical cycling. Regardless, the level of precision observed for these measurements (~8% R.S.D.) is suitable for comparison with alternative systems, as described below.

Comparison with Theory and Alternate Systems. The performance of the new DMF voltammetry cell was compared with that of a commercially available screen-printed electrode (SPE) cell. The DropSens DRP-223AT was chosen for this comparison, as it (like the DMF cell) comprises gold working and auxiliary electrodes and a silver reference electrode. In addition, SPE cells are not mechanically polishable and are typically replaced after fouling. We envision similar usage for the DMF system. Reduction and reoxidation of potassium hexacyanoferrate(III) was used for comparative tests, as this system is known to exhibit nearly ideal reversible redox behavior (allowing the isolation of electrode effects from the response of the redox couple). This system is expected to produce a voltammogram with reduction and oxidation peaks of equal height, separated by 58 mV (at 25 °C), with the peak currents obeying the Randles-Sevcik equation

$$i_p = (2.68 \times 10^8) n^{3/2} A C \sqrt{D \nu}$$

where i_p is the peak current in amperes, n is the number of electrons transferred in the reaction, A is the area of the electrode in m², C is the concentration of the analyte in mol/L, D is the diffusion coefficient in m²/s, and ν is the scan rate in V/s.²³ These ideal values are expected to hold true for moderate scan rates where the electron transfer kinetics are fast relative to the scan rate and deviations from ideal behavior may be evidence of decreased electron transfer rates caused by electrode fouling or uncompensated solution resistance (the solution resistance between the reference and working electrodes).²⁴

Cyclic voltammetry of potassium hexacyanoferrate(III) in the DMF electrochemical cell resulted in an oxidation/reduction peak height ratio of 0.91 and a peak separation of 87 mV. Because mechanical polishing of the electrodes is not possible, variation from the ideal parameters is not unexpected. When similar measurements were performed using the DRP-223AT

SPE system, an oxidation/reduction peak height ratio of 0.98 and a peak separation of 93 mV was observed (Figure 3A). The

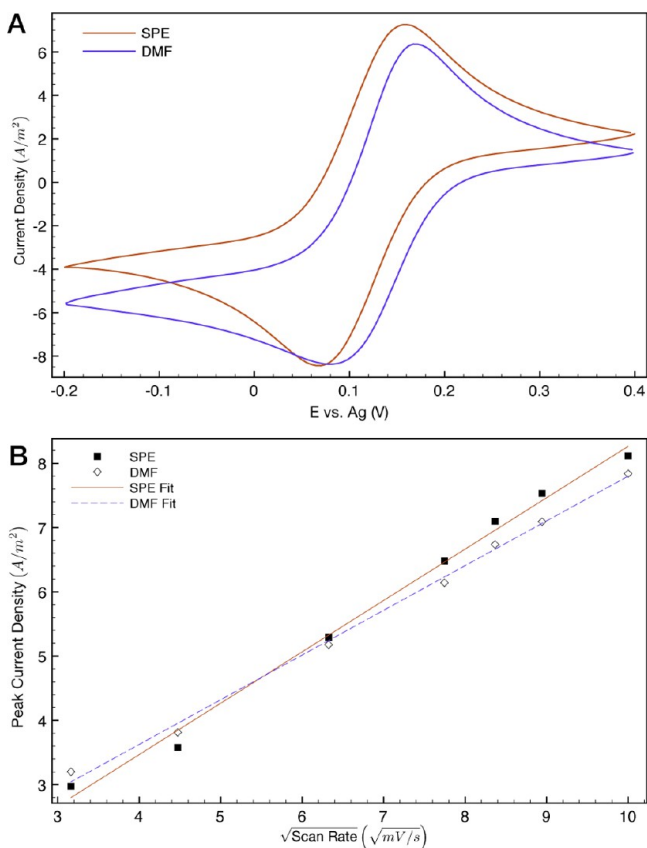


Figure 3. Comparison of cyclic voltammetric analysis of 5 mM potassium hexacyanoferrate(III) in pH 7 McIlvaine buffer using a DMF electrochemical cell and a commercially available screen printed electrode (SPE) cell. (A) Voltammograms at 100 mV/s starting at high potential for the DMF (blue) and SPE (red) cells. (B) Plot of oxidation peak current density as a function of the square root of the scan rate on the SPE (measured data: black squares, fit: solid line) and DMF (data: white diamonds, fit: dashed line) cells.

peak current densities for both systems were approximately linear as a function of the square root of the scan rate, as expected from the Randles-Sevcik equation when all variables apart from the scan rate are constant, resulting in ordinary least-squares fit equations of $y = 0.8425 + 0.6957x$ with an RMS error of 0.096 A/m² for the DMF electrodes and $y = 0.2703 + 0.7994x$ with an RMS error of 0.15 A/m² for the SPE cell (Figure 3B). The cell responses are similar, indicating that the DMF and SPE cells are comparable in performance.

The ideal parameters discussed above are contingent on an electrochemically reversible reaction subject to semi-infinite diffusion to the electrode surface and a planar electrode where radial diffusion is not a significant contributor. To characterize these effects, the diffusion length of ferricyanide in the DMF electrochemical cell was approximated²⁵ to be $l \approx (Dt)^{1/2} \approx 25 \mu\text{m}$, where t is the time-scale of the experiment (1.7 s from the onset of reduction to the peak current) and D is the diffusion coefficient of ferricyanide calculated from the SPE data using the Randles-Sevcik eq ($3.6 \times 10^{-10} \text{ m}^2/\text{s}$). Both the spacing between the top and bottom plates of the device ($\sim 180 \mu\text{m}$) and the diameter of the working electrode ($300 \mu\text{m}$) are within 1 order of magnitude of the diffusion length and may

contribute to deviations from the ideal parameters. In addition, the working electrode is recessed $8 \mu\text{m}$ into the dielectric layer, altering diffusion near the electrode edges, and is spaced $70 \mu\text{m}$ from the counter electrode, so some contribution from redox recycling (i.e., analyte that is oxidized or reduced at the working electrode, diffuses to the counter electrode, is returned to its original state and diffuses back to the working electrode) may be present. While these deviations from ideal conditions do not appear to have a large impact on the measurements reported here, device geometry might be altered to correct for them in the future if measurement of an analyte is adversely affected.

A direct comparison with the previously reported^{10,11} (nonintegrated) DMF/voltammetry systems is not possible, as they were applied to other (more specialized) analytes, but, in general terms, the CV scan rate dependence of the new system is comparable to that of the Karuwan et al.¹⁰ system. Most importantly, the new droplet manipulation capabilities of the system described here (including droplet dispensing from reservoirs) makes it well-suited for sophisticated, multistep processing regimens with minimal human intervention, as described below.

Integrated Quantitative Analysis. The new DMF voltammetry method was applied to analyzing acetaminophen, motivated by the widespread need for rapid analysis of this over-the-counter drug (acetaminophen overdose is a leading cause of acute liver failure cases in the United States²⁶). As shown in Figure 4, a method was developed to generate a dilution series by progressively diluting a droplet of standard acetaminophen solution with diluent. A five-point calibration series (spanning a 5-fold calibration range) required only two pipet steps (loading the standard and diluent reservoirs, respectively) in ~ 18 min. In routine experiments, two dilution series were generated from two different starting concentrations in an experiment requiring a total of three pipet steps to extend the linear dynamic range. This low level of user intervention (two or three pipet steps) contrasts with the one-plate DMF/voltammetry systems reported previously^{10,11} (which are incapable of droplet dispensing or splitting) for which every solution to be evaluated must be prepared manually, off-chip.

In initial experiments, it was observed that when a unit droplet was driven across the (hydrophilic) electrochemical cell, a subdroplet was spontaneously formed (estimated to be $\sim 92 \text{ nL}$) which remained on the cell. This phenomenon is called “passive dispensing” and has been described in detail elsewhere.¹² From repeated voltammetric measurements, it was determined that three successive passive dispensing operations onto the electrochemical cell were sufficient to completely displace the contents of the initial droplet, which agrees with the previous report by Barbulovic-Nad et al.²⁷ Thus, at the beginning of any new experiment, two sample droplets were driven across the electrochemical cell to prime the detector and remove residual analyte from previous experiments prior to delivering the sample droplet to be analyzed (Figure 4A). After the initial measurement, a droplet of diluent was dispensed and delivered to the sample droplet (Figure 4B), and the combined droplet was mixed and returned to the electrochemical cell for analysis (Figure 4C). Dilution, mixing, and measurement steps were then repeated to generate a calibration curve.

The method described above was designed to minimize variance in analyte concentration, which primarily originates from imprecise dispensing of unit droplets (in the device used here, dispensed droplet volumes varied by 2–4% RSD). Thus, in designing the scheme described above, we avoided using the

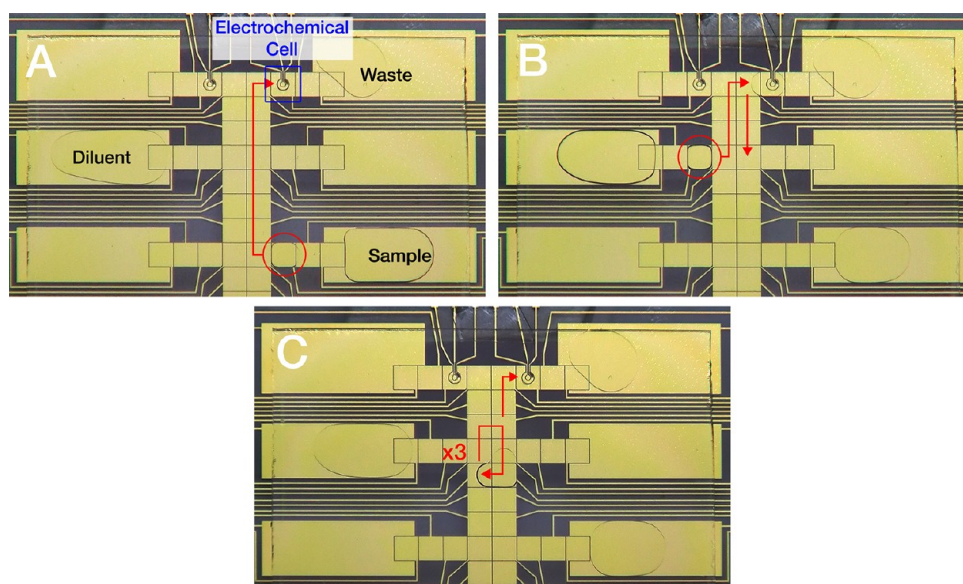


Figure 4. Sequence of frames from a movie illustrating the generation of a dilution series of acetaminophen coupled with analysis by linear sweep voltammetry. (A) Sample droplet dispensed and moved to the electrochemical cell for analysis. (B) Diluent droplet dispensed, moved to merge with the sample droplet, and then moved to general purpose area. (C) Combined droplet mixed and returned to the cell for analysis.

method recently reported by Shih et al.²⁸ (for unrelated applications) which comprised (i) dispensing a unit droplet of diluent from a reservoir, merging it with a unit droplet of media, (ii) splitting the merged droplet, and storing one of the mixed/split droplets to continue the series for further dilution. In this previous method, the variance in two dispensing/splitting steps [(i) and (ii)] contributes to the error in each new diluted concentration, and this error is compounded in subsequent diluted (unit droplet) volume. In contrast, in the new method reported here, because the volume errors in each successive dilution are summed in quadrature, the relative error in the total volume decreases as droplets are added. The new method is not perfect, of course – a practical size-limit is imposed on the number of dilution steps (after five dilutions, the merged droplet becomes impractical to move and measure), and a small, concentration-dependent systematic error is introduced by the depletion of analyte with each voltammetric scan (estimated as ~ 800 nM or 0.2% for the most dilute sample measured). But for the application and goals described here, the new method has excellent analytical performance, as described below.

As shown in the inset to Figure 5, when droplets containing acetaminophen (formed on-chip, as described above) were evaluated by linear sweep voltammetry, distinct peaks at ~ 650 mV were observed, corresponding to the two-electron oxidation of acetaminophen to N-acetyl-4-benzoquinone imine.²⁹ As expected for this diffusion-limited system, the peak current was proportional to acetaminophen concentration and ordinary least-squares regression with three sample replicates yielded a linear fit line with the equation $y = 0.02723 + 0.17481x$ and an RMS error of $0.0081 \mu\text{A}$ (Figure 5 main panel). The reproducibilities of the measurements were excellent, with average relative standard deviations (RSD) of 4% for all concentrations tested. The variance of the blank signal was calculated from repeated measurements of buffer solution ($n = 8$), resulting in a limit of detection (LOD) of $76 \mu\text{M}$ and a limit of quantitation (LOQ) of $130 \mu\text{M}$. While higher than some other voltammetric methods for acetaminophen

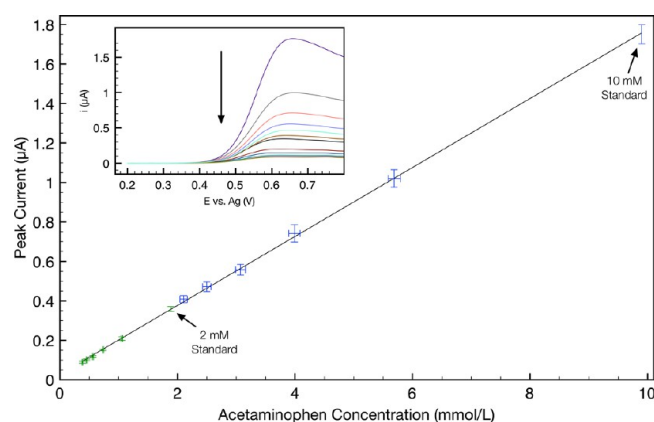


Figure 5. Voltammetric analysis of dilutions of acetaminophen formed on-chip. Calibration curve (main panel) formed from three replicates of five dilutions of 10 mM (blue) and 2 mM (green) acetaminophen standards. X- and Y-error bars are ± 1 s.d. representing estimated volume error from droplet dispensing and current variance between replicates, respectively. Inset: linear sweep voltammograms of acetaminophen droplets on a DMF device at 70 mV/s in pH 3 McIlvaine buffer. Arrow indicates decreasing concentration.

detection,^{30,31} these limits are comparable to those of the fluorescence polarization immunoassays that are commonly used to quantify serum acetaminophen concentrations (reported to be suitable for concentrations above $330 \mu\text{M}$ ³²) and are comfortably lower than the 1.3 mM concentration-cutoff used to diagnose hepatic damage.³³

Analysis by voltammetry is relatively rare in the microfluidic literature. Most microchannel/electrochemistry systems used for quantitative measurement reported previously have used amperometry,^{34–39} which is useful for rapid detection of bands of analytes as they flow through channels. For voltammetric measurements in such systems, the sample solution must reside in proximity to the electrodes for enough time to scan a range of potentials,⁴⁰ which poses challenges for techniques like flow injection analysis and limits flexibility in sample handling. In

practice, this requires special techniques capable of slow or reversed flow,^{41,42} no flow,^{43–45} or very rapid scanning.⁴² We posit that the digital microfluidic format (whether operated electrically as is the case here or magnetically as described elsewhere⁴⁶) is uniquely suited to analysis by voltammetry, as it facilitates seamless transition between (mobile) sample delivery and (stationary) sample analysis.

In future work, we note that device fabrication is not limited to producing electrochemical electrodes from gold or silver (as described here). In principle, any conductive material may be used to construct DMF electrodes and electrodes composed of any metal capable of thin film deposition on the substrate and patterning by photolithography could be produced for the new design reported here. Alternate electrode materials could expand the use of this and similar devices to applications including biosensors and environmental measurements.

CONCLUSION

A two-plate digital microfluidic platform with integrated electrochemical cells for voltammetry was produced using standard microfabrication techniques. The cell, based upon gold working and counter electrodes and a silver reference electrode, was characterized by cyclic voltammetry of hexacyanoferrate(III) and was found to have comparable performance to a commercial screen printed electrode cell. The platform was used to generate ten standard solutions of acetaminophen by repeated dilution and was measured using linear sweep voltammetry with minimal human intervention, resulting in a detection limit suitable for the quantification of acetaminophen for overdose testing. The combination of digital microfluidics with voltammetric measurement represents a versatile system for microscale analysis of many analytes.

AUTHOR INFORMATION

Corresponding Author

*Phone: (416) 946 3864. Fax: (416) 946 3865. E-mail: aaron.wheeler@utoronto.ca.

Notes

The authors declare no competing financial interest.

ACKNOWLEDGMENTS

We thank the Canadian Institutes for Health Research (CIHR) for financial support and Shana Kelley (Univ. Toronto) for helpful discussions. M.D.M.D. thanks the Natural Sciences and Engineering Research Council of Canada (NSERC) for a scholarship, and A.R.W. thanks the Canada Research Chair (CRC) Program for a CRC.

REFERENCES

- (1) Jones, T. B. *Langmuir* **2002**, *18*, 4437–4443.
- (2) Choi, K.; Ng, A. H. C.; Fobel, R.; Wheeler, A. R. *Annu. Rev. Anal. Chem.* **2012**, *5*, 413–440.
- (3) Jebraïl, M.; Assem, N.; Mudrik, J.; Dryden, M.; Lin, K.; Yudin, A.; Wheeler, A. R. *J. Flow Chem.* **2012**, *2*, 103–107.
- (4) Boles, D. J.; Benton, J. L.; Siew, G. J.; Levy, M. H.; Thwar, P. K.; Sandahl, M. A.; Rouse, J. L.; Perkins, L. C.; Sudarsan, A. P.; Jalili, R.; Pamula, V. K.; Srinivasan, V.; Fair, R. B.; Griffin, P. B.; Eckhardt, A. E.; Pollack, M. G. *Anal. Chem.* **2011**, *83*, 8439–8447.
- (5) Abdelgawad, M.; Watson, M. W. L.; Wheeler, A. R. *Lab Chip* **2009**, *9*, 1046–1051.
- (6) Srinivasan, V.; Pamula, V. K.; Fair, R. B. *Lab Chip* **2004**, *4*, 310–315.

- (7) Sista, R.; Hua, Z.; Thwar, P.; Sudarsan, A.; Srinivasan, V.; Eckhardt, A.; Pollack, M.; Pamula, V. *Lab Chip* **2008**, *8*, 2091–2104.
- (8) Malic, L. L.; Veres, T. T.; Tabrizian, M. M. *Lab Chip* **2009**, *9*, 473–475.
- (9) Kirby, A. E.; Wheeler, A. R. *Lab Chip* **2013**, *13*, 2533–2540.
- (10) Karuwan, C.; Sukthang, K.; Wisitsoraat, A.; Phokharatkul, D.; Patthanasettakul, V.; Wechsato, W.; Tuantranont, A. *Talanta* **2011**, *84*, 1384–1389.
- (11) Dubois, P.; Marchand, G.; Fouillet, Y.; Berthier, J.; Douki, T.; Hassine, F.; Gmouh, S.; Vaultier, M. *Anal. Chem.* **2006**, *78*, 4909–4917.
- (12) Eydelnant, I. A.; Uddayasankar, U.; Li, B.; Liao, M. W.; Wheeler, A. R. *Lab Chip* **2012**, *12*, 750–757.
- (13) Ng, A. H. C.; Choi, K.; Luoma, R. P.; Robinson, J. M.; Wheeler, A. R. *Anal. Chem.* **2012**, *84*, 8805–8812.
- (14) Fobel, R.; Fobel, C.; Wheeler, A. R. *Appl. Phys. Lett.* **2013**, *102*, 193513–193518.
- (15) Trasatti, S.; Petrii, O. A. *J. Electroanal. Chem. (Lausanne, Switz.)* **1992**, *327*, 353–376.
- (16) McIlvaine, T. C. *J. Biol. Chem.* **1921**, *49*, 183–186.
- (17) Ku, H. H. *J. Res. Natl. Bur. Stand., Sect. C* **1966**, *70C*, 263.
- (18) Malic, L.; Veres, T.; Tabrizian, M. *Biosens. Bioelectron.* **2009**, *24*, 2218–2224.
- (19) Fischer, L. M.; Tenje, M.; Heiskanen, A. R.; Masuda, N.; Castillo, J.; Bentien, A.; Émneus, J.; Jakobsen, M. H.; Boisen, A. *Microelectron. Eng.* **2009**, *86*, 1282–1285.
- (20) Bott, A. W. *Curr. Sep.* **1995**, *14*, 64–69.
- (21) Kinlen, P. J.; Heider, J. E.; Hubbard, D. E. *Sens. Actuators, B* **1994**, *22*, 13–25.
- (22) Ghilane, J.; Hapiot, P.; Bard, A. J. *Anal. Chem.* **2006**, *78*, 6868–6872.
- (23) Harris, D. C. *Quantitative Chemical Analysis*, 7th ed.; W. H. Freeman: New York, 2007.
- (24) Mabbott, G. A. *J. Chem. Educ.* **1983**, *60*, 697.
- (25) Scholz, F. *Electrochemical Dictionary*; Springer: Berlin/Heidelberg, DEU, 2008.
- (26) Ostapowicz, G. *Ann. Intern. Med.* **2002**, *137*, 947.
- (27) Barbulovic-Nad, I.; Au, S. H.; Wheeler, A. R. *Lab Chip* **2010**, *10*, 1536–1542.
- (28) Shih, S. C. C.; Barbulovic-Nad, I.; Yang, X.; Fobel, R.; Wheeler, A. R. *Biosens. Bioelectron.* **2013**, *42*, 314–320.
- (29) Nematollahi, D.; Shayani-Jam, H.; Alimoradi, M.; Niroomand, S. *Electrochim. Acta* **2009**, *54*, 7407–7415.
- (30) Jia, L.; Zhang, X. H.; Li, Q.; Wang, S. F. *J. Anal. Chem.* **2007**, *62*, 266–269.
- (31) Goyal, R.; Gupta, V.; Oyama, M.; Bachheti, N. *Electrochem. Commun.* **2005**, *7*, 803–807.
- (32) Edinboro, L. E.; Jackson, G. F.; Jortani, S. A.; Poklis, A. *Clin. Toxicol.* **1991**, *29*, 241–255.
- (33) Rumack, B. H.; Peterson, R. G. *Pediatrics* **1978**, *62*, 898–903.
- (34) Gunasekara, D. B.; Hulvey, M. K.; Lunte, S. M. *Electrophoresis* **2011**, *32*, 832–837.
- (35) Liu, H.; Crooks, R. M. *Lab Chip* **2013**, *13*, 1364–1370.
- (36) Selimovic, A.; Johnson, A. S.; Kiss, I. Z.; Martin, R. S. *Electrophoresis* **2011**, *32*, 822–831.
- (37) Amatore, C.; Da Mota, N.; Sella, C.; Thouin, L. *Anal. Chem.* **2008**, *80*, 4976–4985.
- (38) Chikkaveeraiah, B. V.; Liu, H.; Mani, V.; Papadimitrakopoulos, F.; Rusling, J. F. *Electrochem. Commun.* **2009**, *11*, 819–822.
- (39) Sassa, F.; Morimoto, K.; Satoh, W.; Suzuki, H. *Electrophoresis* **2008**, *29*, 1787–1800.
- (40) Yunus, K.; Fisher, A. C. *Electroanalysis* **2003**, *15*, 1782–1786.
- (41) Dunchai, W.; Chailapakul, O.; Henry, C. S. *Anal. Chem.* **2009**, *81*, 5821–5826.
- (42) Wang, J.; Polsky, R.; Tian, B.; Chatrathi, M. P. *Anal. Chem.* **2000**, *72*, 5285–5289.
- (43) Chainani, E. T.; Ngo, K. T.; Scheeline, A. *Anal. Chem.* **2013**, *85*, 2500–2506.

- (44) Triroj, N.; Lapierre-Devlin, M. A.; Kelley, S. O.; Beresford, R. *IEEE Sens. J.* **2006**, *6*, 1395–1402.
- (45) Pavlovic, E.; Lai, R. Y.; Wu, T. T.; Ferguson, B. S.; Sun, R.; Plaxco, K. W.; Soh, H. T. *Langmuir* **2008**, *24*, 1102–1107.
- (46) Lindsay, S.; Vázquez, T.; Egatz-Gómez, A.; Loyprasert, S.; Garcia, A. A.; Wang, J. *Analyst* **2007**, *132*, 412–416.